THE STUDY OF THE BEHAVIOUR OF DIFFRACTIVE STRUCTURE FUNCTIONS

SARA TAHERI MONFARED
ALI KHORRAMIAN

Semnan University &
School of particles and accelerators,
Institute for Research in Fundamental Science (IPM)

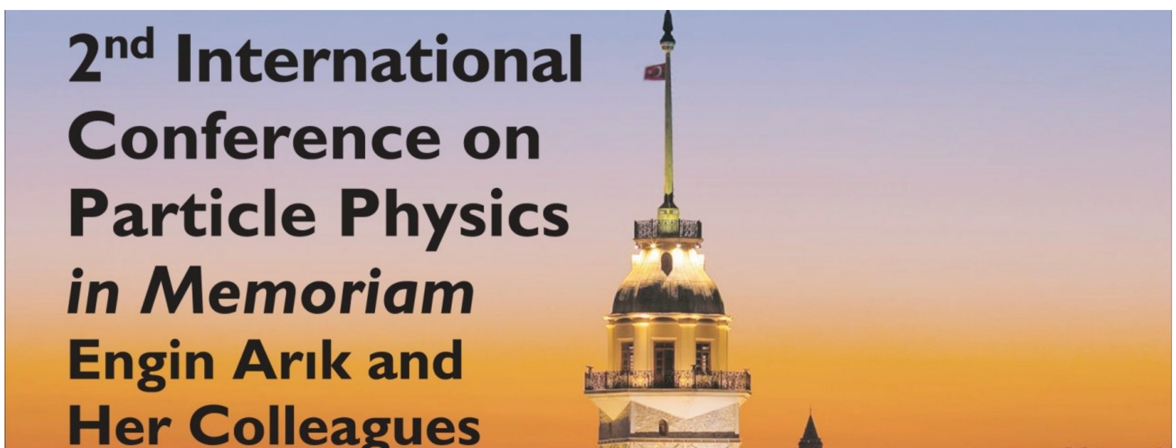

THE STUDY OF THE BEHAVIOUR OF DIFFRACTIVE STRUCTURE FUNCTIONS

- **Motivation**
- **DDIS kinematics**
- **Introduction of different diffractive data sets**
- **Global fit procedure**
- **Results and conclusion**

Motivation

Structure functions are a measure of the partonic structure of hadrons, which is important for any process which involves colliding hadrons. **They are key ingredient for deriving PDFs in nucleons**. These PDFs allow us to predict cross sections at particle colliders and a good knowledge of PDFs is of prime importance for the success of the physics program.

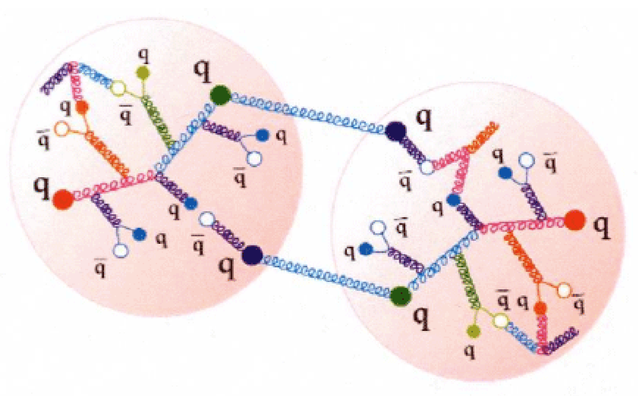

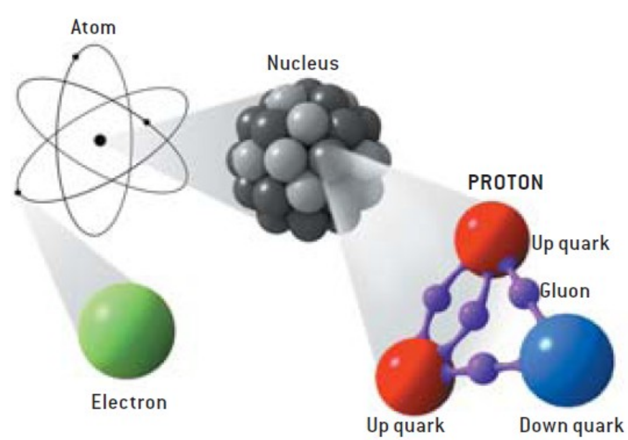

A. De Roeck and R. S. Thorne, arXiv:1103.0555 [hep-ph].

M. G. Albrow *et al.* [FP420 R and D Collaboration], JINST **4**, T10001 (2009) [arXiv:0806.0302 [hep-ex]].

The H1 and ZEUS collaborations presented their results on inclusive and various exclusive reactions, which is being actively studied by theorists and give access to a broader understanding of proton structure. **Although data-taking there has been stopped, new results continue to appear.**

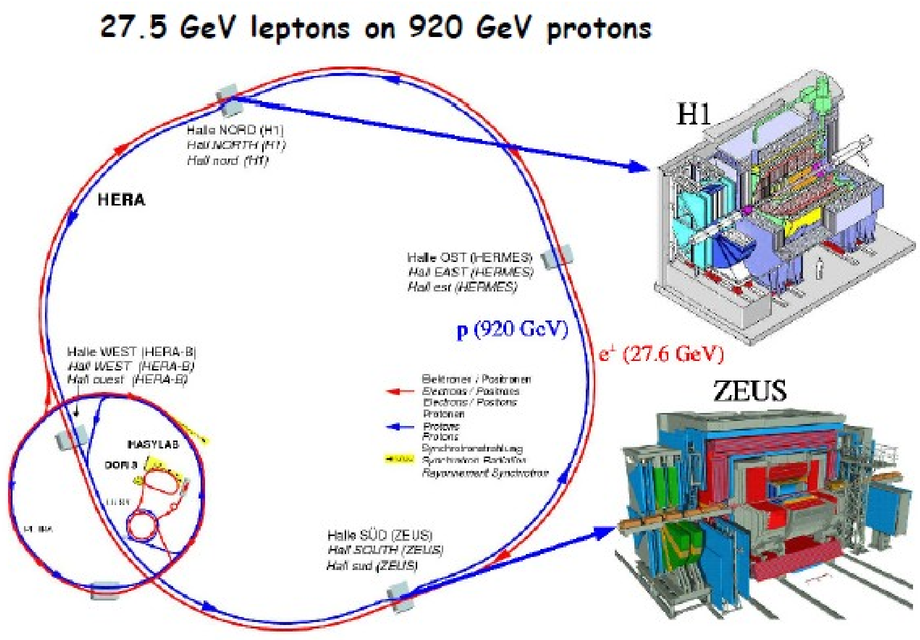

H. Collaboration, arXiv:1010.1476 [hep-ex].

In order that we might develop better understanding of the DDIS phenomena, I am first going to begin with a short introduction to DIS phenomena which testifies itself as the basis of the former.

Standard DIS

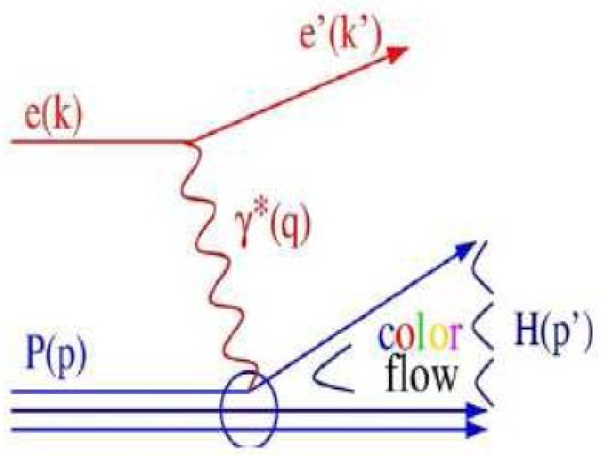

The deep-inelastic lepton-nucleon scattering is the source of important information about the nucleons structure.

DDIS

Now let's focus our attention on the main theme of today's talk, DDIS.

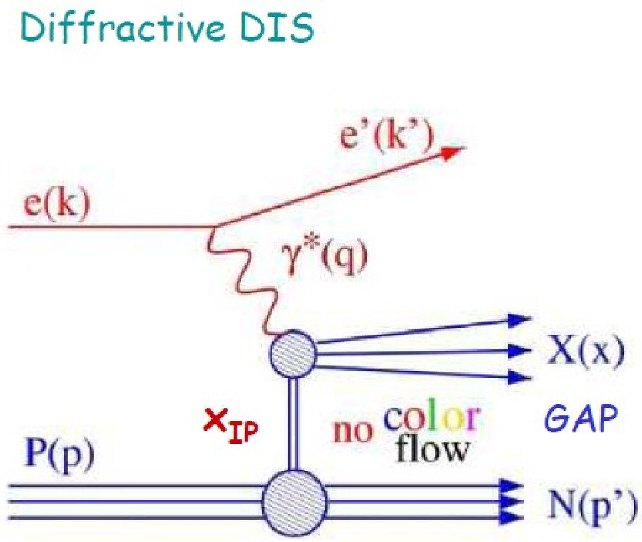

•Approximately 10% of DIS phenomena are of diffractive nature.

•Diffractive DIS is an ideal laboratory to study the interface of perturbative and non-perturbative physics in the QCD.

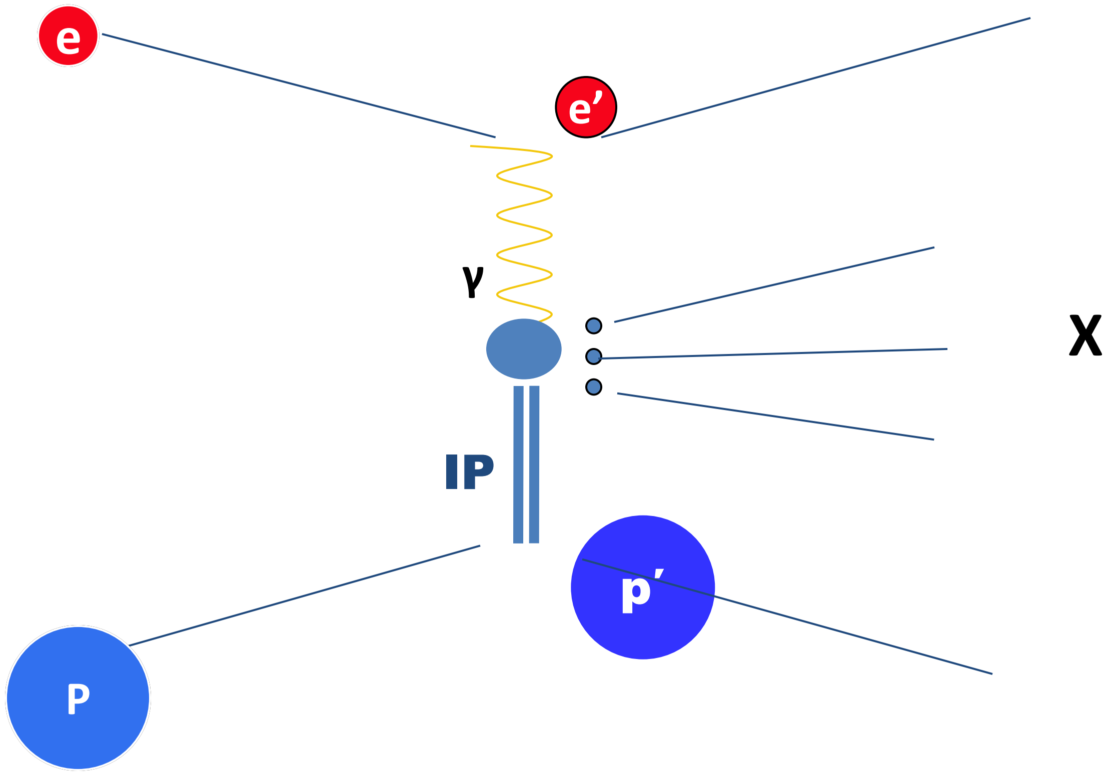

Diffractive events are characterized by the fact that the incoming proton(s) emerge from the interaction intact, or are excited into a low mass state, with only a small energy loss. Diffractive processes are mediated by an exchange with quantum numbers of the vacuum, the so-called Pomeron (IP) now understood in terms of partons from the proton.

Before the proper analysis we need to define the usual kinematic variables. The main variables used for the description of DDIS are similar to DIS variable.

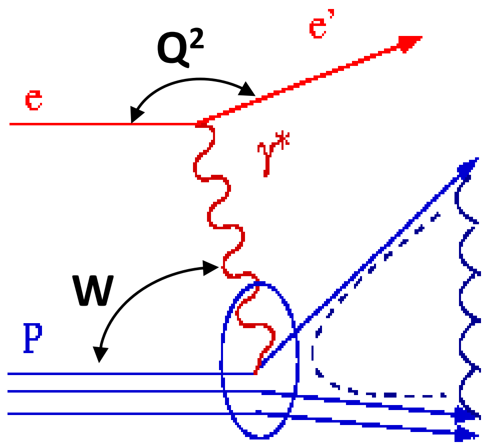

Q^2 = virtuality of photon
=(4-momentum exchanged at e vertex)^2

W = invariant mass of photon-proton system

x = Bjorken's variable for the Proton
= fraction of Proton's momentum carried by struck quark

y = inelasticity

$$\frac{d^2\sigma}{dxdQ^2} = \frac{4\pi\alpha^2}{xQ^4}\left\{1 - y + \frac{y^2}{2[1 + R(x,Q^2)]}\right\} \underline{F_2(x,Q^2)}$$

A. N. Khorramian, S. Atashbar Tehrani, S. Taheri Monfared, F. Arbabifar and F. I. Olness, Phys. Rev. D **83**, 054017 (2011) [arXiv:1011.4873 [hep-ph]].

A. N. Khorramian, H. Khanpour and S. A. Tehrani, Phys. Rev. D **81**, 014013 (2010) [arXiv:0909.2665 [hep-ph]].

A. N. Khorramian and S. A. Tehrani, Phys. Rev. D **78**, 074019 (2008) [arXiv:0805.3063 [hep-ph]].

DIS probes the partonic structure of the proton

The variables related to DDIS bear a close resemblance to those of DIS.

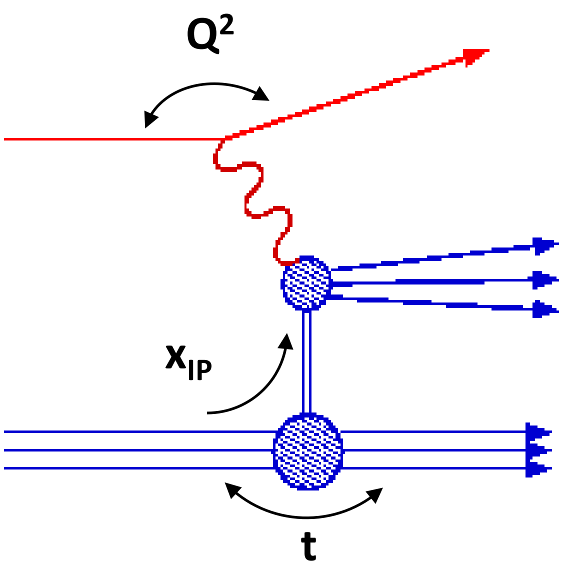

x_{IP} = fraction of proton's momentum taken by Pomeron

β = Bjorken's variable for the Pomeron
= fraction of Pomeron's momentum carried by struck quark
= x/x_{IP}

t = (4-momentum exchanged at p vertex)^2
typically: $|t| < 1\text{GeV}^2$

M_X = invariant mass of photon-Pomeron system

$$\frac{d^4\sigma}{d\beta dQ^2 dx_{IP} dt} = \frac{4\pi\alpha^2}{\beta Q^4}\left\{1 - y + \frac{y^2}{2(1+R^{D(4)})}\right\} F_2^{D(4)}(\beta, Q^2, x_{IP}, t)$$

Diffractive Selection Methods and Data Sets Considered

How the data are presented

There is no unique definition of a cross section for DDIS. Different methods exist to select diffractive events.

1. These methods select samples which contain different fractions of proton dissociative events. Cross sections are usually given without corrections for proton dissociation.

2. A second problem originates from the fact that also non-diffractive events may contain a rapidity gap due to the statistical nature of fragmentation or from the exchange of Reggeon. Such rapidity gaps are, however, exponentially suppressed.

Three distinct methods have been employed by the HERA experiments, which select inclusive diffractive events.

All data sets are transported to the H1-LRG measureament range M_Y <1.6 GeV^2.

M_X Method:

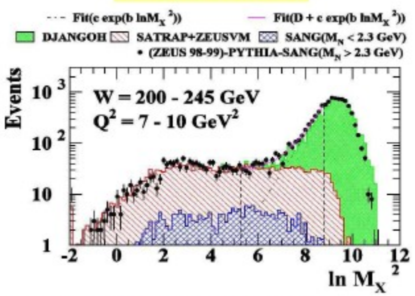

- Flat (vs) ln M_X^2 for diffractive events
- Non diffractive events substracted from fits
  → Small proton dissociation contamination
  → No access to t

M_Y >2.3 GeV^2
Scaling factor 0.86

M_Y <1.6 GeV^2
Scaling factor 1.03
For ZEUS

Large Rapidity Gap (LRG) Method:

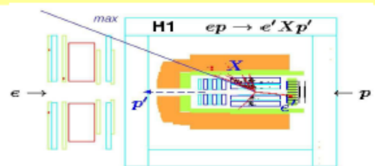

- Request LRG in main detector (3.3<η<7.5)
- Meassure kinematic from e$^\pm$ and X system
  → No access to t
- Some proton dissociation contamination
  → Corrected up to M_Y < 1.6 GeV

Tagged Leading Baryons Method:

H1 (FPS) and ZEUS (LPS) have Proton Spectrometers (and Forward Neutron Calorimeters)

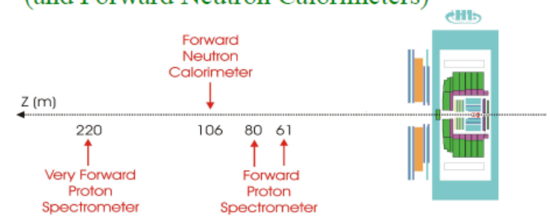

- Free of proton dissociation background
- Proton 4-momentum measurement → t, x_{IP}
- Lower statistic (acceptance)

M_Y =M_P GeV^2
Scaling factor 1.33,1.20

The full HERA data sample analysis is a powerful technique to achieve the best precision possible in extracting DPDFs.

Published data points

Lable	Data set	β-range	x_{IP}-range	Q^2-range [GeV^2]	of data points	Ref.	Multiplying factor
H1-LRG-06	$\sigma_r^{D(3)}$	0.0043-0.8	0.001-0.03	8.5-1600	190	[1]	
H1-FPS-06	$\sigma_r^{D(3)}$	0.02-0.7	0.0011-0.08	10.7-24	40	[2]	1.23
ZEUS-M_X-05	$F_2^{D(3)}$	0.0153-0.75	0.00048-0.02126	14-55	56	[3]	0.86
ZEUS-LPS-04	$F_2^{D(3)}$	0.007-0.48	0.0005-0.06	13.5-39	27	[4]	1.33
ZEUS-M_X-08	$F_2^{D(3)}$	0.021-0.799	0.0006-0.03345	14-320	244	[5]	0.86
ZEUS-LRG-09	$\sigma_r^{D(3)}$	0.025-0.7955	0.0005-0.014	8.5-225	155	[6]	1.03
ZEUS-LPS-09	$\sigma_r^{D(3)}$	0.013-0.609	0.0009-0.09	14-40	42	[6]	1.2
H1-FPS-10	$\sigma_r^{D(3)}$	0.0056-0.562	0.0025-0.075	8.8-200	100	[7]	1.2
total					854		

Table 1: Published data points □ < 0.8, $M_x > 2$ GeV and $Q^2 > 8.5$ GeV^2, in order to avoid regions which are most likely to be influenced by higher twist contributions.

[1] A. Aktas *et al.* [H1 Collaboration], Eur. Phys. J. C **48**, 715 (2006) [arXiv:hep-ex/0606004].

[2] A. Aktas *et al.* [H1 Collaboration], Eur. Phys. J. C **48**, 749 (2006) [arXiv:hep-ex/0606003].

[3] S. Chekanov *et al.* [ZEUS Collaboration], Eur. Phys. J. C **38**, 43 (2004) [arXiv:hep-ex/0408009].

[4] S. Chekanov *et al.* [ZEUS Collaboration], Nucl. Phys. B **713**, 3 (2005) [arXiv:hep-ex/0501060].

[5] S. Chekanov *et al.* [ZEUS Collaboration], Nucl. Phys. B **816**, 1 (2009) [arXiv:0812.2003 [hep-ex]].

[6] S. Chekanov [ZEUS Collaboration], Nucl. Phys. B **800**, 1 (2008) [arXiv:0802.3017 [hep-ex]].

[7] H. Collaboration, arXiv:1010.1476 [hep-ex].

Diffractive Parton Distribution Functions

This is equivalent to treating the diffractive exchange as a pomeron with a partonic structure given by the parton distributions and the pomeron flux factor representing the probability that a pomeron with particular values of x_{IP} and t couples to the proton.

$$f_i^D(x, Q^2, x_{IP}, t) = f_{IP/p}(x_{IP}, t) \cdot f_i^{IP}(\beta = x/x_{IP}, Q^2)$$

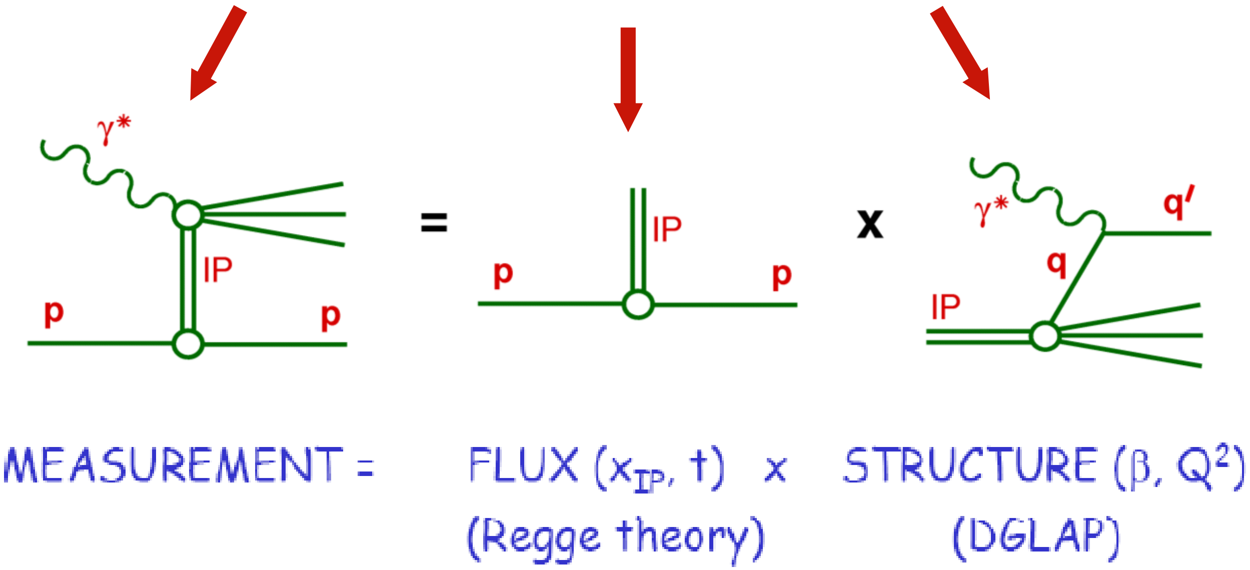

C. Royon, L. Schoeffel, J. Bartels, H. Jung and R. B. Peschanski, Phys. Rev. D **63**, 074004 (2001) [arXiv:hep-ph/0010015].

The DPDFs are modeled in terms of a singlet distribution $\Sigma(z)$, consisting of u, d and s quarks and anti-quarks with $u = d = s = \bar{u} = \bar{d} = \bar{s}$, and a gluon distribution g(z). The quark singlet and gluon distributions are parameterized at the starting scale Q_0^2 as:

Pomeron Parton Distribution function

We step into the process of this project by performing a QCD fit under the same conditions and conventions as in H12006. Then we tried to vary □ distribution functional form to improve our fitting procedure.

H1 parameterization form

$$z\Sigma(z,Q_0^2) = A_\Sigma z^{B_\Sigma}(1-z)^{C_\Sigma} e^{\frac{a=-0.01}{1-z}}$$

Fit A

$$zg(z,Q_0^2) = A_g (1-z)^{C_g} e^{\frac{a=-0.01}{1-z}}$$

Fit B

$$zg(z,Q_0^2) = A_g e^{\frac{a=-0.01}{1-z}}$$

Our form

$$z\Sigma(z,Q_0^2) = A_\Sigma z^{B_\Sigma}(1-z)^{C_\Sigma}(1 + D_\Sigma z + E_\Sigma z^{F_\Sigma})$$

$$zg(z,Q_0^2) = A_g e^{\frac{a=-0.01}{1-z}}$$

It ensures that the distribution vanish at z=1, as required for evolution equation to be solvable.

Please note that our Model reduces □2 significantly.

A. Aktas *et al.* [H1 Collaboration], Eur. Phys. J. C 48, 715 (2006) [arXiv:hep-ex/0606004].

F_L^D can be neglected anywhere but at large y due to the presence of y^2/Y_+.

$$\sigma_r^{D(3)} = F_2^{D(3)} - \frac{y^2}{Y_+} F_L^{D(3)}$$

$$Y_+ = 1 + (1-y)^2$$

The effect of F_L^D are considered through its relation to the NLO parton densities, such that no explicit cut on y is required.

$$sxy = Q^2$$

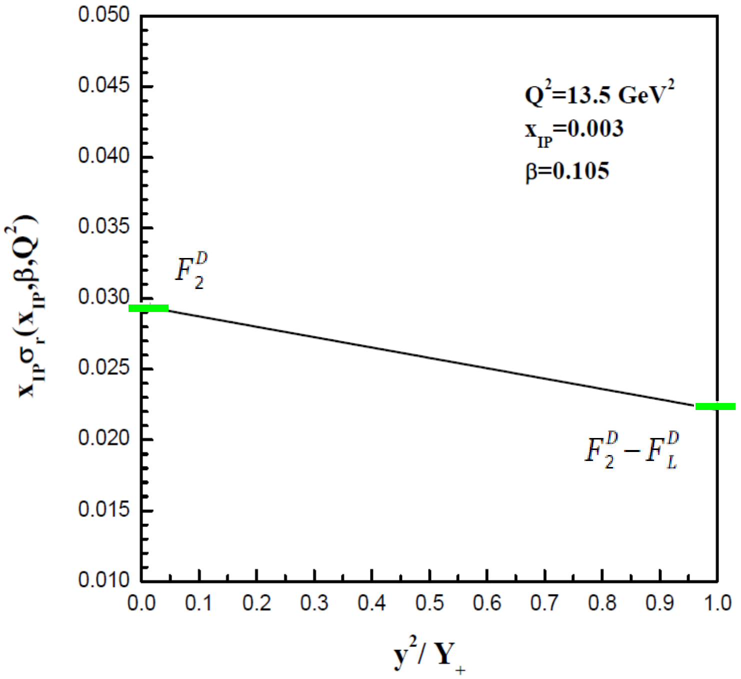

Highest sensitivity to F_L at high y (low □)

How to get a better result

To obtain a good description of the data, an additional sub-leading exchange (IR) is included, which contributes significantly only at low β and large x_{IP}. this contribution is assumed to factorize in the same way as the pomeron term, such that the evaluation of DPDFs becomes:

IP component

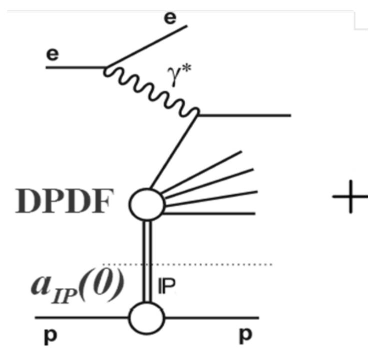

component

$$f_i^D(\beta, Q^2, x_{IP}, t) \quad = \quad f_{IP/p}(x_{IP}, t) \cdot f_i(\beta, Q^2)$$

Our final results

Parameters	All data sets
A_Σ	0.15 ± 0.007
B_Σ	0.02 ± 0.028
C_Σ	0.54 ± 0.023
D_Σ	5.16 ± 0.147
E_Σ	-2.39 ± 0.070
F_Σ	0.30 ± 0.014
A_g	0.36 ± 0.019
α_{IP}	1.118 ± 0.0030
N_{IR}(H1-LRG-06)	$(2.14 \pm 0.16) \times 10^{-3}$
N_{IR}(H1-FPS-06)	$(1.52 \pm 0.22) \times 10^{-3}$
N_{IR}(ZEUS-M_X-05)	-
N_{IR}(ZEUS-LPS-04)	$(1.99 \pm 0.26) \times 10^{-3}$
N_{IR}(ZEUS-M_X-08)	-
N_{IR}(ZEUS-LRG-09)	$(3.35 \pm 0.26) \times 10^{-4}$
N_{IR}(ZEUS-LPS-09)	$(2.15 \pm 0.11) \times 10^{-3}$
N_{IR}(H1-FPS-10)	$(1.75 \pm 0.08) \times 10^{-3}$
χ^2/dof	$925.11/840 = 1.101$

Table 2: Pomeron quark and gluon densities parameters and their statistical errors for combined data sets at the input scale $Q_0^{\ 2}$ =3 GeV^2. No Reggeon contribution is necessary for the M_X data sets.

Our DPDFs

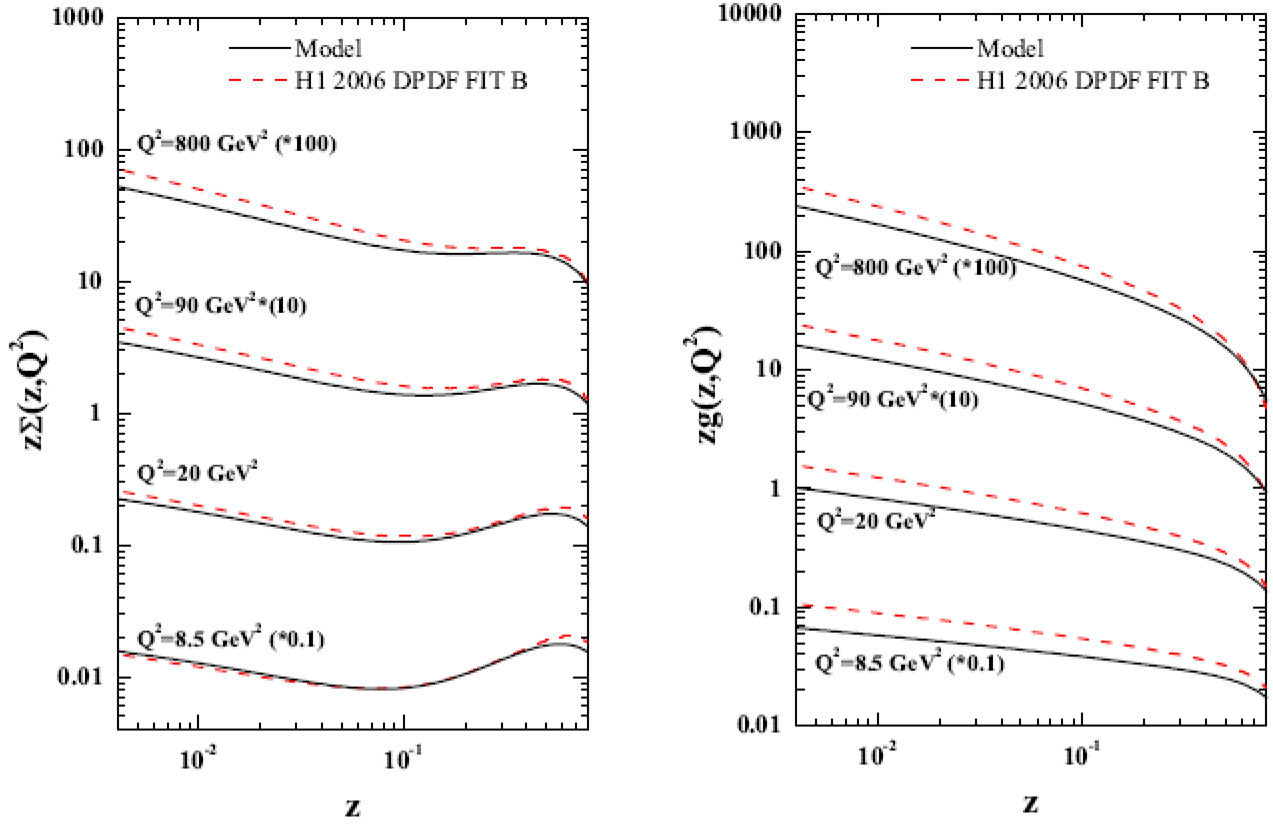

Figure 1: Comparison between the total quark singlet and gluon distributions obtained from our model and H1 2006 DPDF Fit B. The DPDFs are shown at four different values of Q^2 as a function of z.

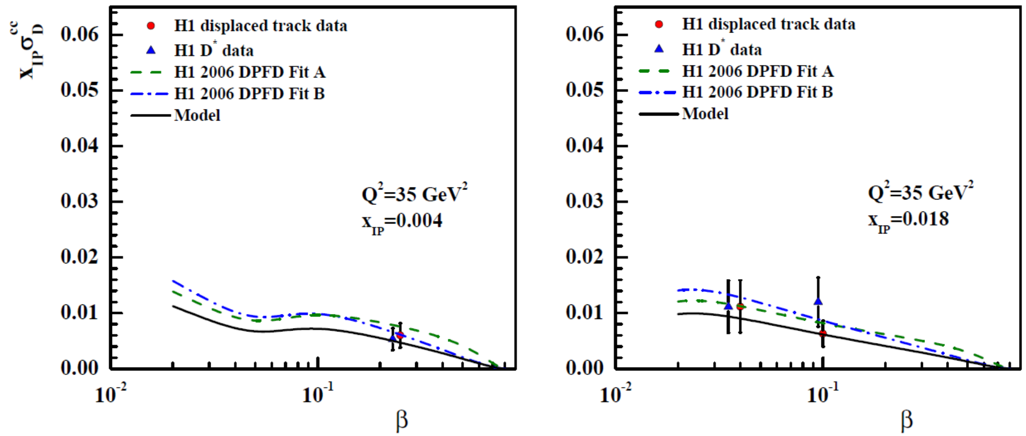

Figure 2: Comparison of our result for the contribution of the charm quarks to the diffractive cross section with H1 DPDF Fit A and Fit B shown as a function of □ for two different values of x_{IP}. The data obtained from the H1 displaced track method and D^* production in DIS.

S. Chekanov *et al.* [ZEUS Collaboration], Nucl. Phys. B **672**, 3 (2003) [arXiv:hep-ex/0307068].

A. Aktas *et al.* [H1 Collaboration], Eur. Phys. J. C **50**, 1 (2007) [arXiv:hep-ex/0610076].

Our result on heavy structure functions

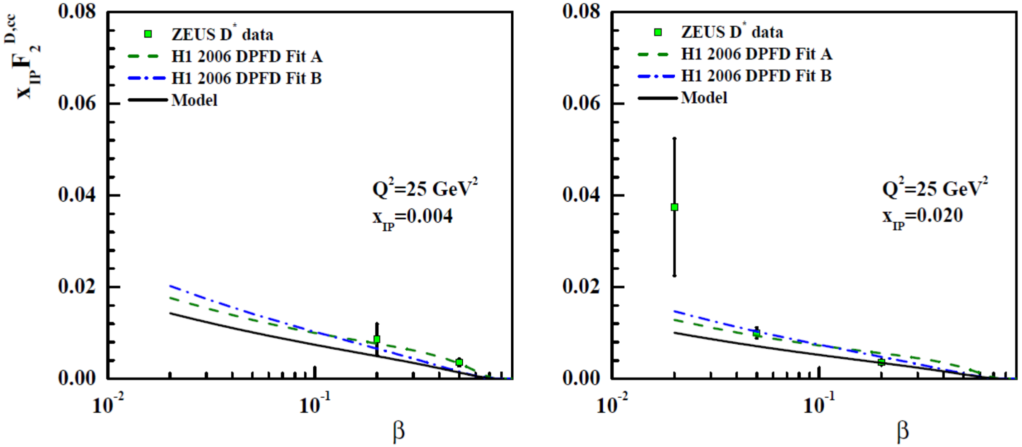

Figure 3: Comparison of our result for the contribution of the charm quarks to the diffractive cross section and structure functions with H1 DPDF Fit A and Fit B shown as a function of □ for two different values of x_{IP}. The data obtained from the ZEUS D^* production in DIS.

S. Chekanov *et al.* [ZEUS Collaboration], Nucl. Phys. B **672**, 3 (2003) [arXiv:hep-ex/0307068].

A. Aktas *et al.* [H1 Collaboration], Eur. Phys. J. C **50**, 1 (2007) [arXiv:hep-ex/0610076].

Behavior of structure function versus □

F_2^D is largely flat in the measured range. Keeping in mind the similarity between □ in diffractive DIS and x_{Bj} in inclusive DIS, this is very different from the behavior of the usual structure function F_2, which strongly decreases for $x_{Bj} > 0.2$.

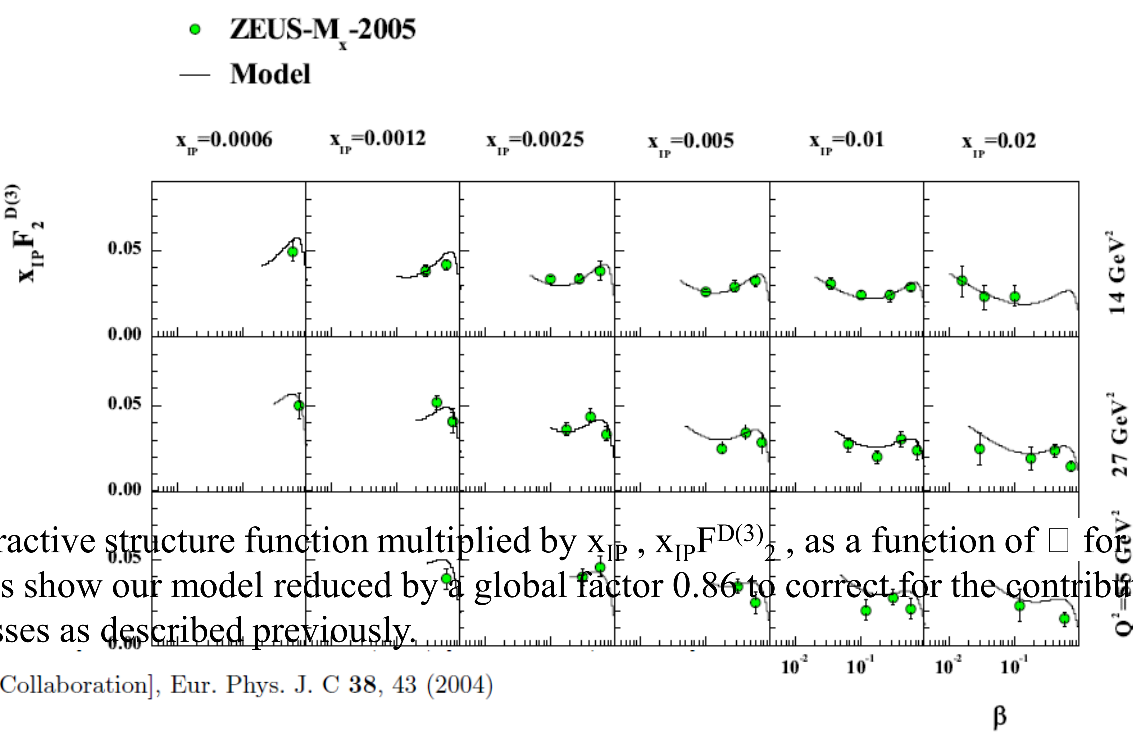

Figure 4: The diffractive structure function multiplied by x_{IP} , $x_{IP}F^{D(3)}_2$, as a function of □ for different regions of Q^2 and x_{IP} . The curves show our model reduced by a global factor 0.86 to correct for the contributions of proton dissociation processes as described previously.

S. Chekanov *et al.* [ZEUS Collaboration], Eur. Phys. J. C **38**, 43 (2004) [arXiv:hep-ex/0408009].

F_2^D increases with Q^2 for all □ values except the highest. This is reminiscent of the scaling violations of F_2, except that F_2 rises with Q^2 only for $x_{Bj} < 0.2$ and that the scaling violations become negative at higher x_{Bj} . In the proton, negative scaling violations reflect the presence of the valence quarks radiating gluons, while positive scaling violations are due to the increase of the sea quark and gluon densities as the proton is probed with higher resolution. **The F_2^D data thus suggest that the partons resolved in diffractive events are predominantly gluons.**

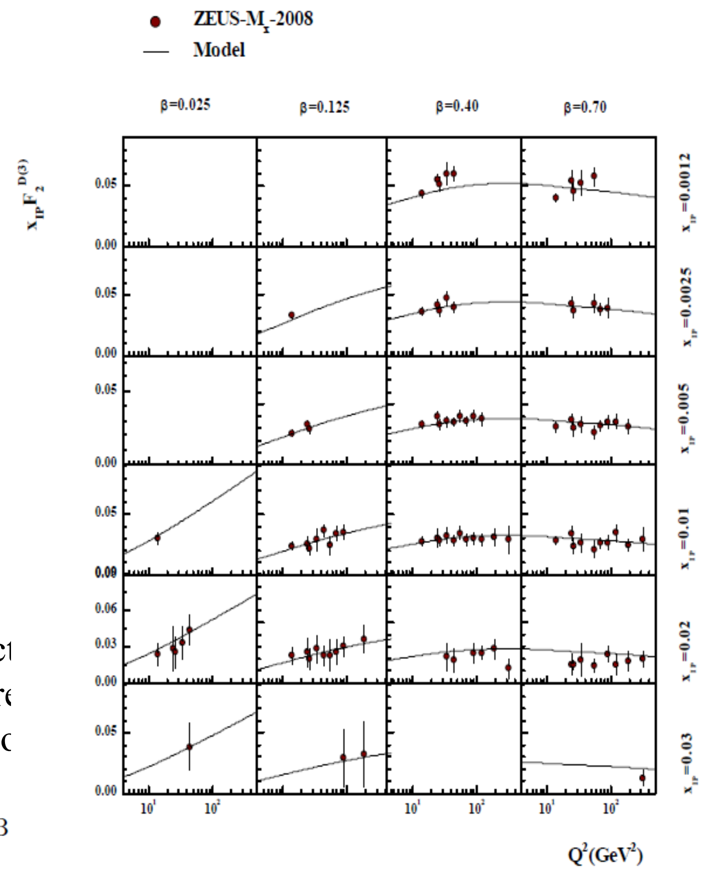

Figure 4: The diffractive cross sect ifferent regions of □ and x_{IP}. The curves show our model re contributions of proton dissc

S. Chekanov *et al.* [ZEUS Collaboration], Nucl. Phys. B [hep-ex]].

QCD Fit – comparison with ZEUS-LPS-04 data

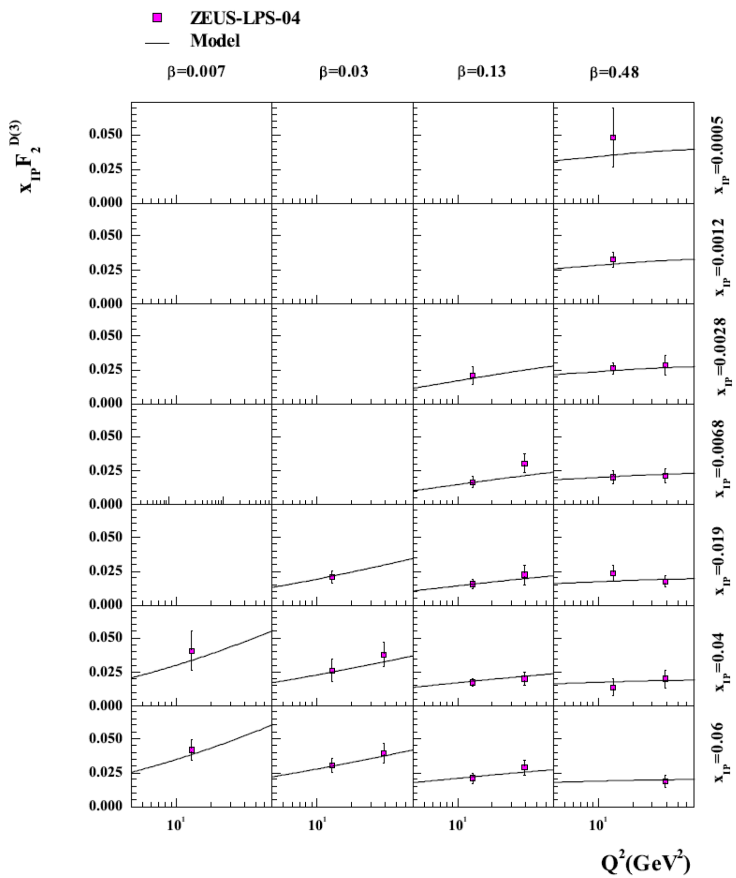

Figure : The diffractive structure function multiplied by x_{IP}, as a function of Q^2 for different regions of □ and x_{IP}. The curves show our model reduced by a global factor 1.33 to correct for the contributions of proton dissociation processes as described previously.

S. Chekanov *et al.* [ZEUS Collaboration], Eur. Phys. J. C **38**, 43 (2004) [arXiv:hep-ex/0408009].

Diffractive cross sections

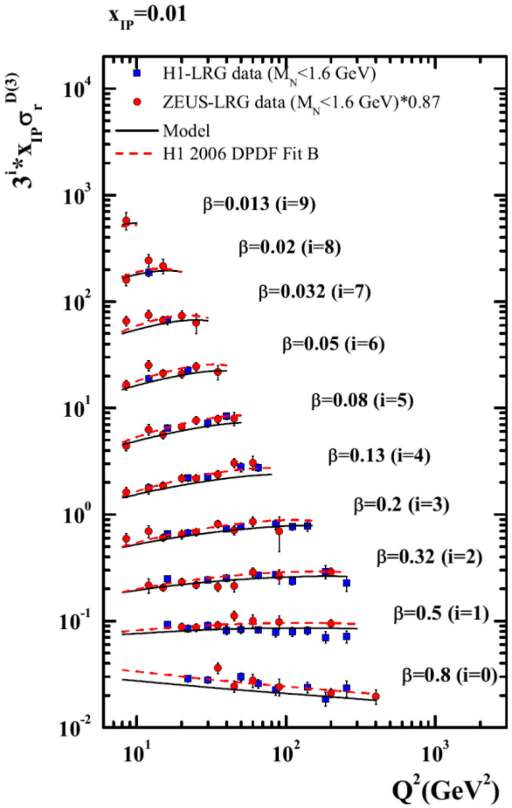

Figure 5: Comparison between the H1 and ZEUS LRG measurements after correcting both data sets to $M_N < 1.6$ GeV in $x_{IP}=0.01$.

A. Aktas *et al.* [H1 Collaboration], Eur. Phys. J. C **48**, 715 (2006) [arXiv:hep-ex/0606004].

S. Chekanov [ZEUS Collaboration], Nucl. Phys. B **800**, 1 (2008) [arXiv:0802.3017 [hep-ex]].

QCD Fit – comparison with LRG data

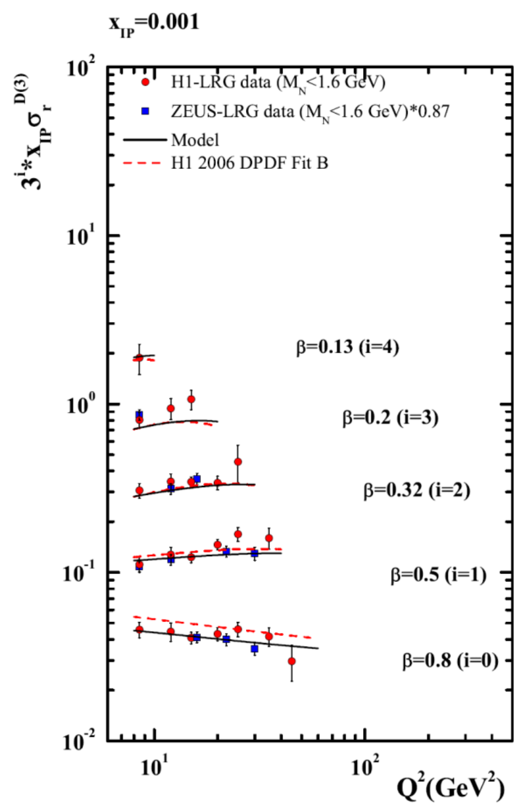

Figure 6: Comparison between the H1 and ZEUS LRG measurements after correcting both data sets to $M_N < 1.6$ GeV in x_{IP}=0.001.

A. Aktas *et al.* [H1 Collaboration], Eur. Phys. J. C **48**, 715 (2006) [arXiv:hep-ex/0606004].

S. Chekanov [ZEUS Collaboration], Nucl. Phys. B **800**, 1 (2008) [arXiv:0802.3017 [hep-ex]].

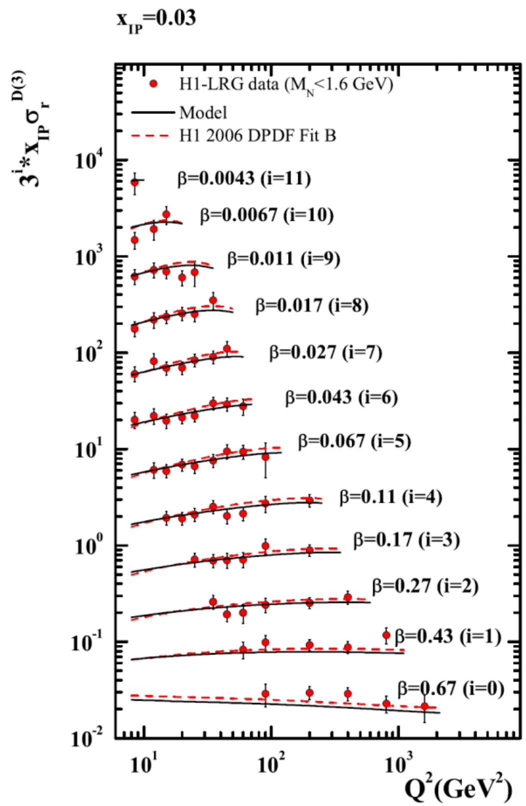

Figure 7: Comparison between the H1 and ZEUS LRG measurements after correcting both data sets to M_N < 1.6 GeV in x_{IP}=0.03.

A. Aktas *et al.* [H1 Collaboration], Eur. Phys. J. C **48**, 715 (2006) [arXiv:hep-ex/0606004].

S. Chekanov [ZEUS Collaboration], Nucl. Phys. B **800**, 1 (2008) [arXiv:0802.3017 [hep-ex]].

QCD Fit – comparison with LRG data

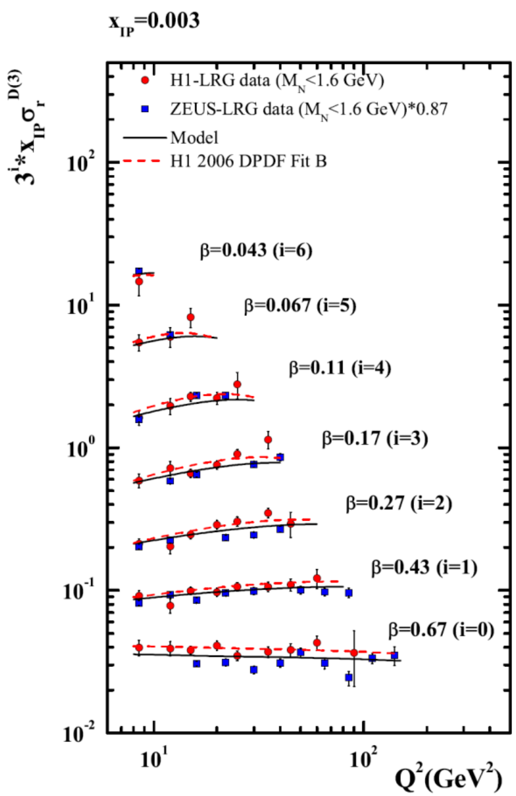

Figure 8: Comparison between the H1 and ZEUS LRG measurements after correcting both data sets to $M_N <$ 1.6 GeV in x_{IP}=0.003.

A. Aktas *et al.* [H1 Collaboration], Eur. Phys. J. C **48**, 715 (2006) [arXiv:hep-ex/0606004].

S. Chekanov [ZEUS Collaboration], Nucl. Phys. B **800**, 1 (2008) [arXiv:0802.3017 [hep-ex]].

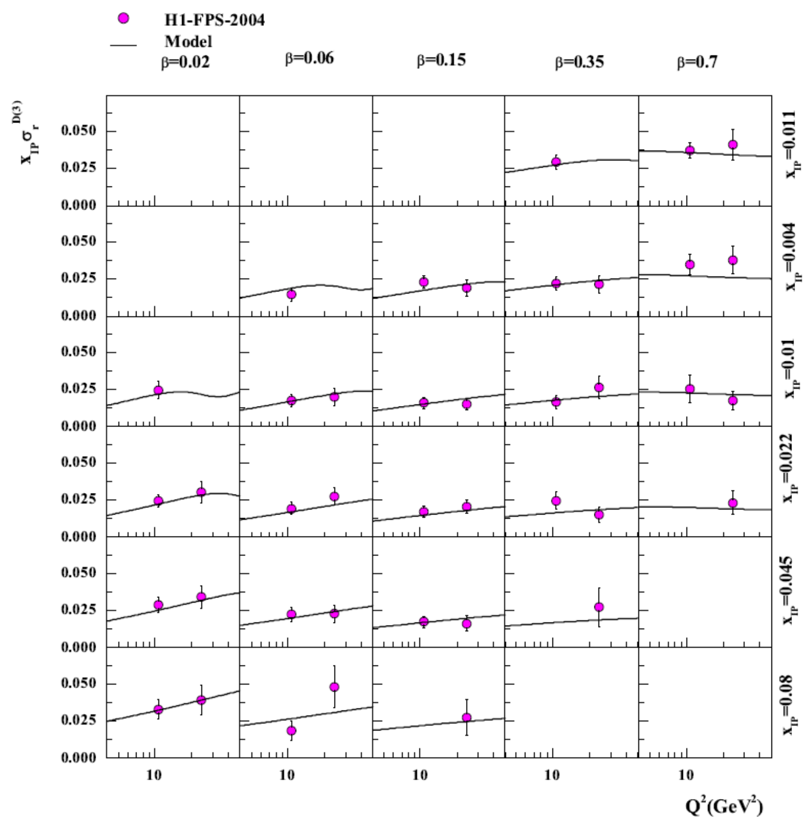

Figure 9: The diffractive cross section multiplied by x_{IP} , as a function of Q^2 for different regions of □ and x_{IP}. The curves show our model reduced by a global factor 1.23 to correct for the contributions of proton dissociation processes as described previously.

A. Aktas *et al.* [H1 Collaboration], Eur. Phys. J. C 48, 749 (2006) [arXiv:hep-ex/0606003].

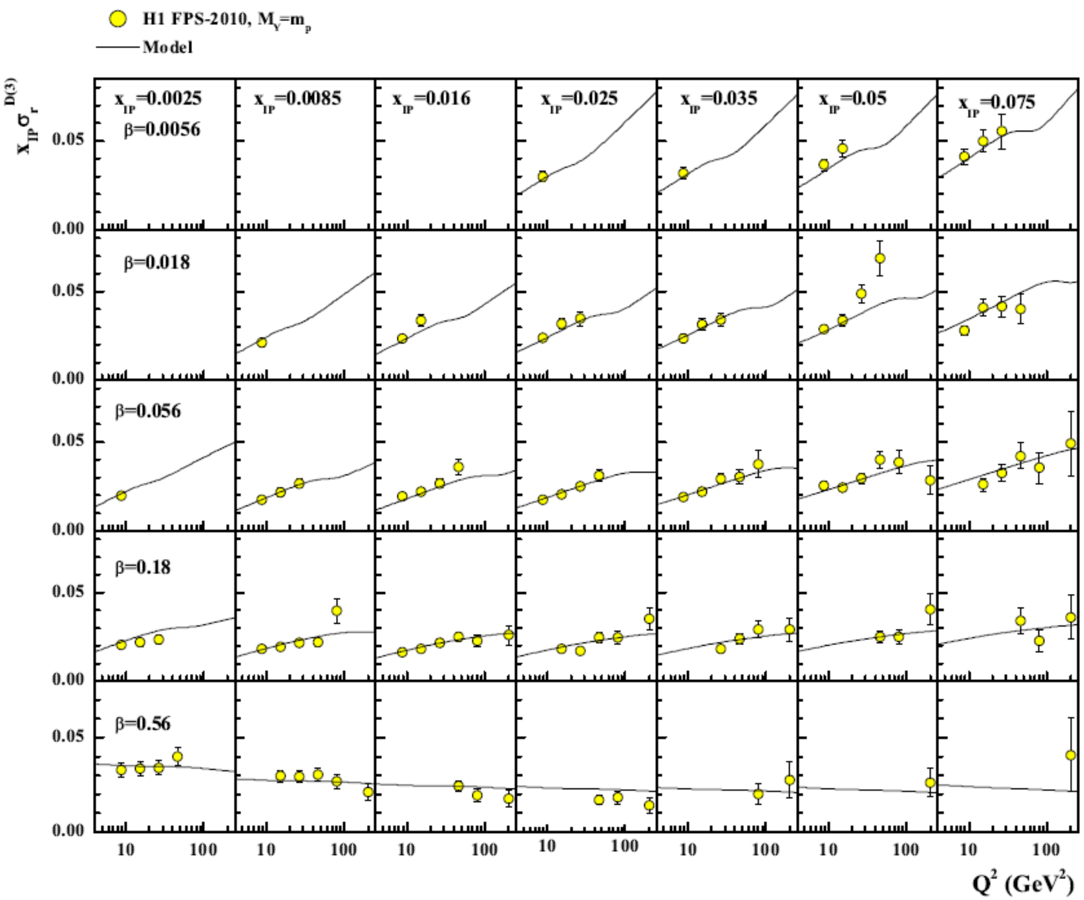

Figure 10: The diffractive cross section multiplied by x_{IP} , as a function of Q^2 for different regions of □ and x_{IP}. The curves show our model reduced by a global factor 1.20 to correct for the contributions of proton dissociation processes as described previously.

H. Collaboration, arXiv:1010.1476 [hep-ex].

Conclusion

In conclusion, this has been a general overview of what really fascinated me through the course of this study.

•We have shown that the diffractive observables measured in the H1 and ZEUS experiments at HERA can be well described by a perturbative QCD analysis which fundamental quark and gluon distributions, evolving according to the NLO DGLAP equations, are assigned to the Pomeron and Reggeon exchanges.

•Although these data obtained by various methods with very different systematic, they are broadly consistent in the shapes of the distribution throughout most of the phase space.

•Although we have not used charm structure function experimental data in fitting procedure, our heavy results are in good agreement with observables.

Thanks for your paying attention

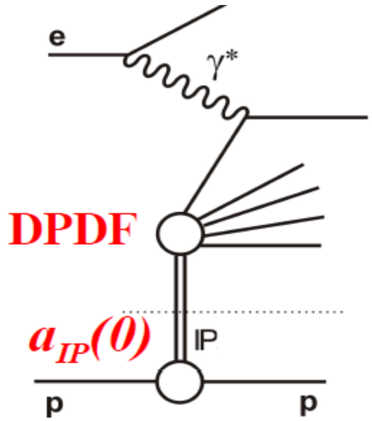

IP component

Secondary IR component

$$f_i^{D(4)} = f_{IP}(x_{IP}, t) \cdot f_i^{IP}(\beta, Q^2)$$

J. Owens, Phys. Rev. D **30** (1984) 943.

QCD Fit – comparison with ZEUS-M_X-05 data

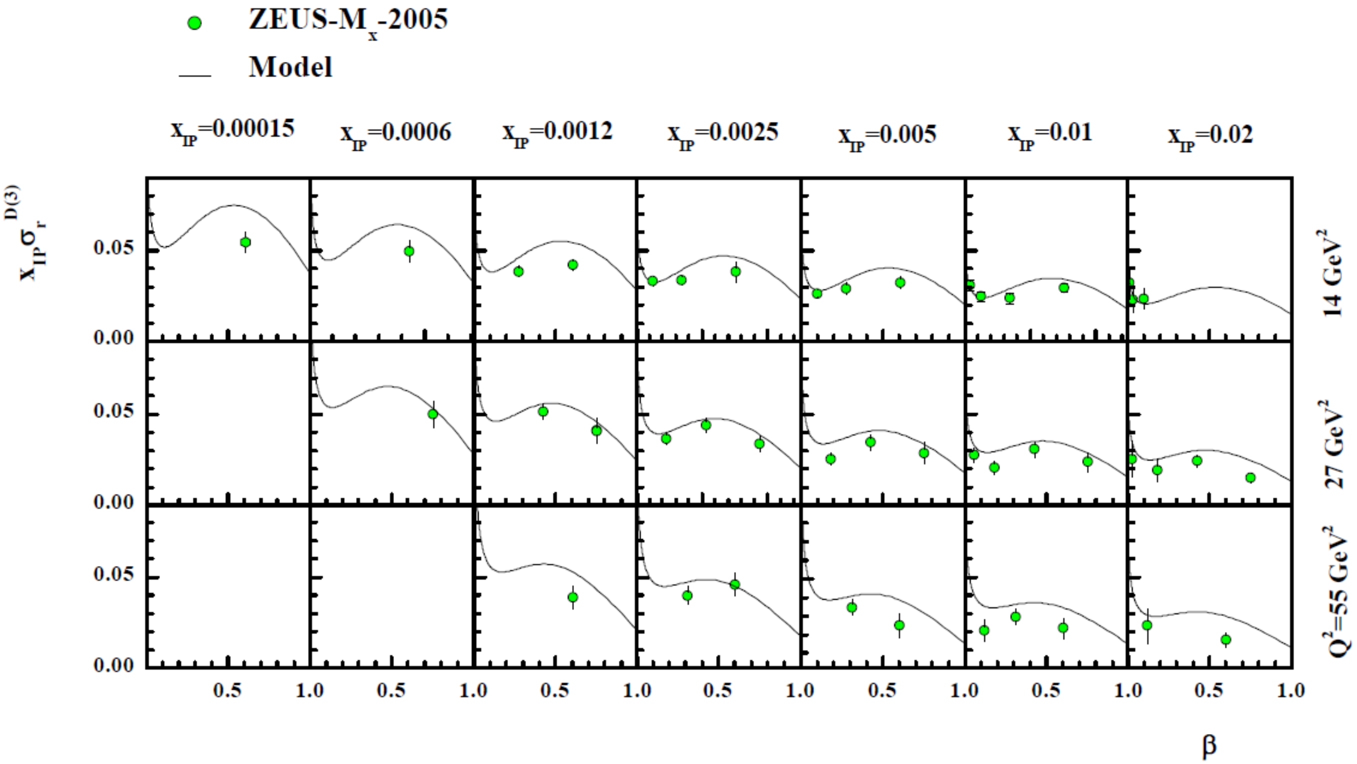

The diffractive cross section of the proton multiplied by x_{IP} , as a function of for different regions of x_{IP} and Q^2. The curves show the result of our fit.

S. Chekanov *et al.* [ZEUS Collaboration], Eur. Phys. J. C **38**, 43 (2004) [arXiv:hep-ex/0408009].

H1 preliminary F^D_L

H1prelim-10-017

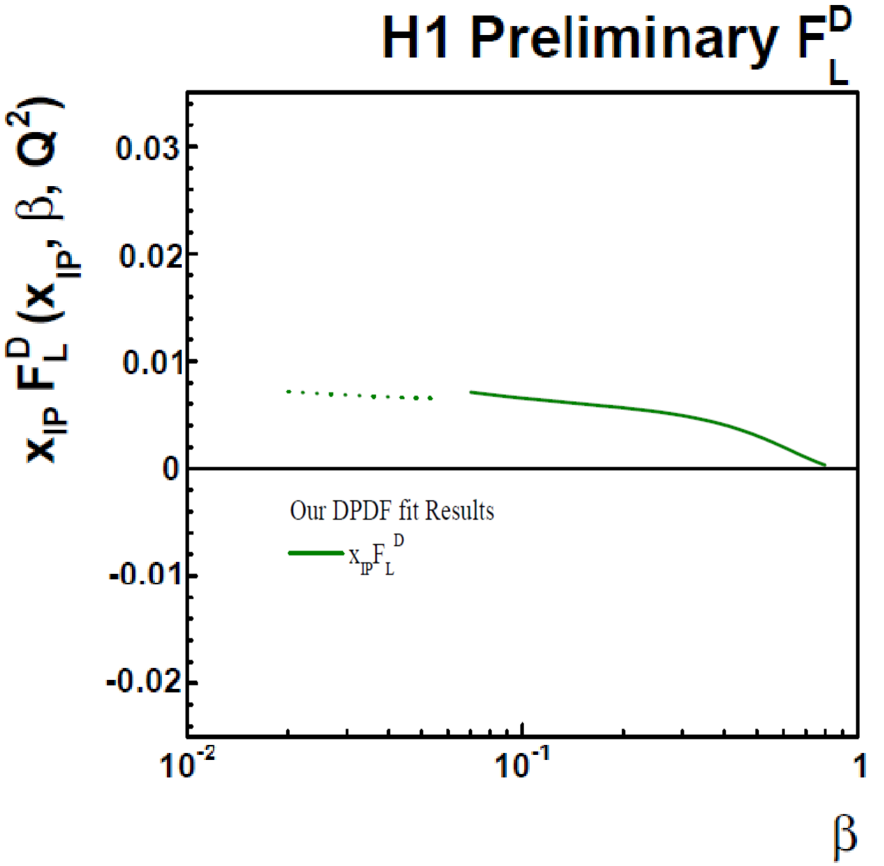

The measured longitudinal reduced cross section obtained from H1 and ZEUS shown as a function of □ for different values of x_{IP}. Our model is compared with H1 2006 DPDF Fit A and B.

Flux factor

Flux factor represents the probability that a pomeron with particular values of x_{IP} and t couples to the proton

$$f_{IP}(x_{IP},t) = A_{IP}\frac{e^{\beta_{IP}t}}{x_{IP}^{2\alpha_{IP}(t)-1}}$$

$$\alpha_{IP}(t) = \alpha_{IP}(0) + \alpha'_{IP}.t$$

$$x_{IP}\cdot\int_{t_{cut}}^{t_{\min}} f_{IP/p}\,dt = 1$$

$$x_{IP} = 0.003$$

$$|t_{\min}| \approx m_p^2 x_{IP}^2/(1-x_{IP})$$

$$|t_{cut}| = 1.0\,GeV^2$$

$$M_x = \sqrt{Q^2(\frac{1}{\beta}-1)}$$

Pomeron

- The pomeron carries no charges. → The absence of electric charge implies that pomeron exchange does not lead to the usual shower of Cherenkov radiation.

- The pomeron carries no colures. → The absence of color charge implies that such events do not radiate pions.

This is in accord with experimental observation. In high energy proton–antiproton collisions in which it is believed that pomerons have been exchanged, a rapidity gap is often observed. This is a large angular region in which no outgoing particles are detected.

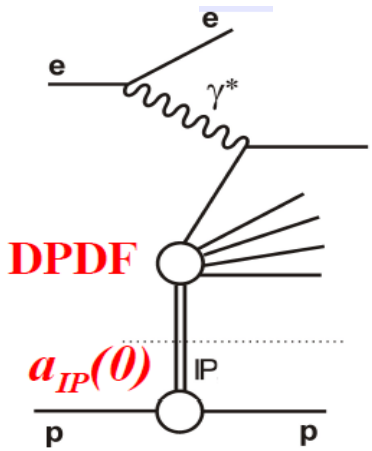

IP component

$$f_i^{D(4)} = f_{IP}(x_{IP}, t) \cdot f_i^{IP}(\beta, Q^2)$$

Secondary IR component

Fit

- $a_{IP}(0)$ (x_{IP} dependence).
- Five parameters of DPDFs (β and Q^2 dependences) using NLO QCD.

Fit

- One parameter for normalization
- The parton densities of sub-leading exchange are taken from pion structure function data

J. Owens, Phys. Rev. D **30** (1984) 943.

M_x Method

$$\frac{dN_{diff}}{dlnM^{۲}} \sim constant,$$

$$\frac{dN_{nondiff}}{dlnM^{۲}} = c.e^{(b.lnM^{۲})}, \quad b > ۰.$$

$$\frac{dN}{dlnM^{۲}} = D + c.e^{(b.lnM^{۲})}, \quad b > ۰.$$

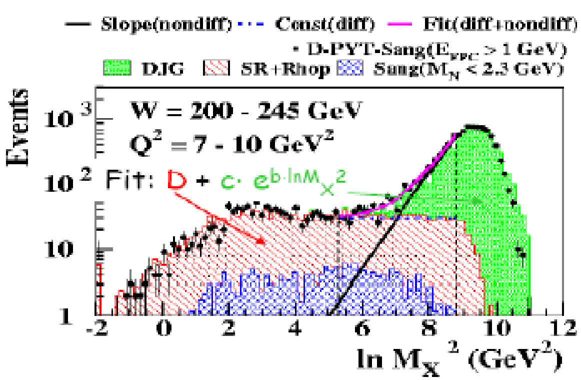

Is F_L a really important part in cross section?

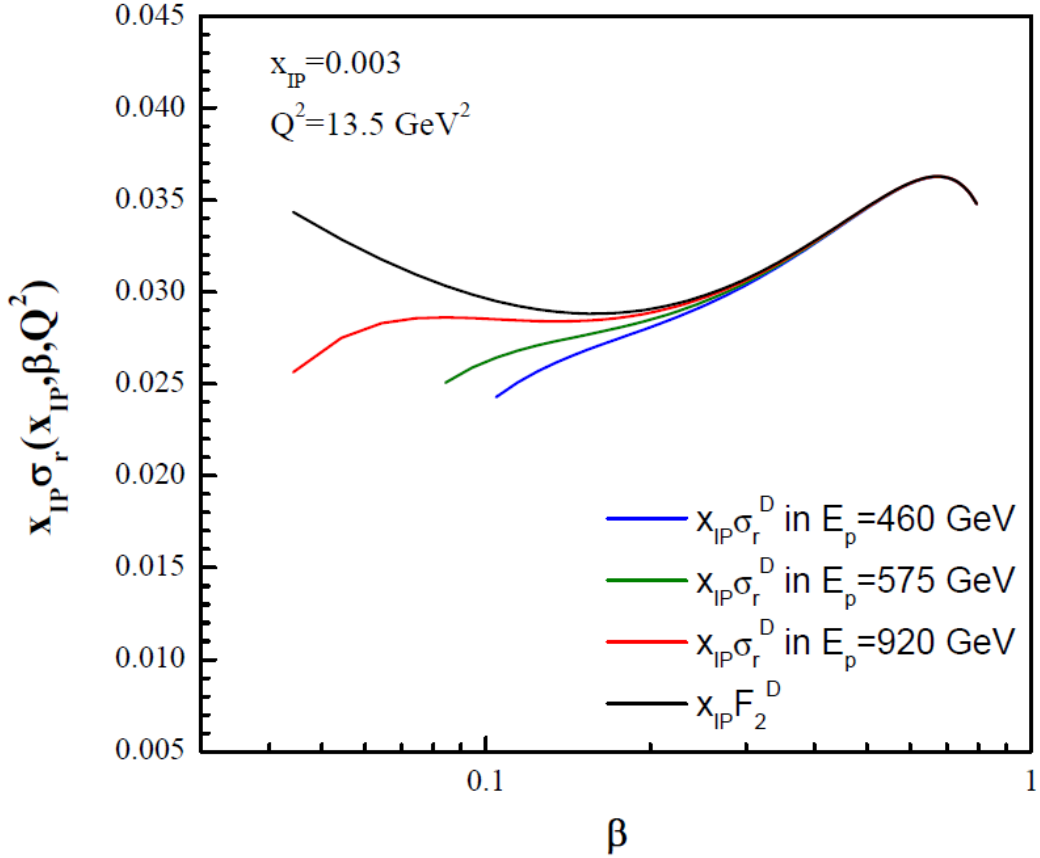

Cross sections are sensitive to F_L .
We considered F_L contributions to perform more precise fitting procedure.

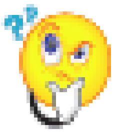

Thanks for
your attention

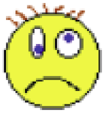

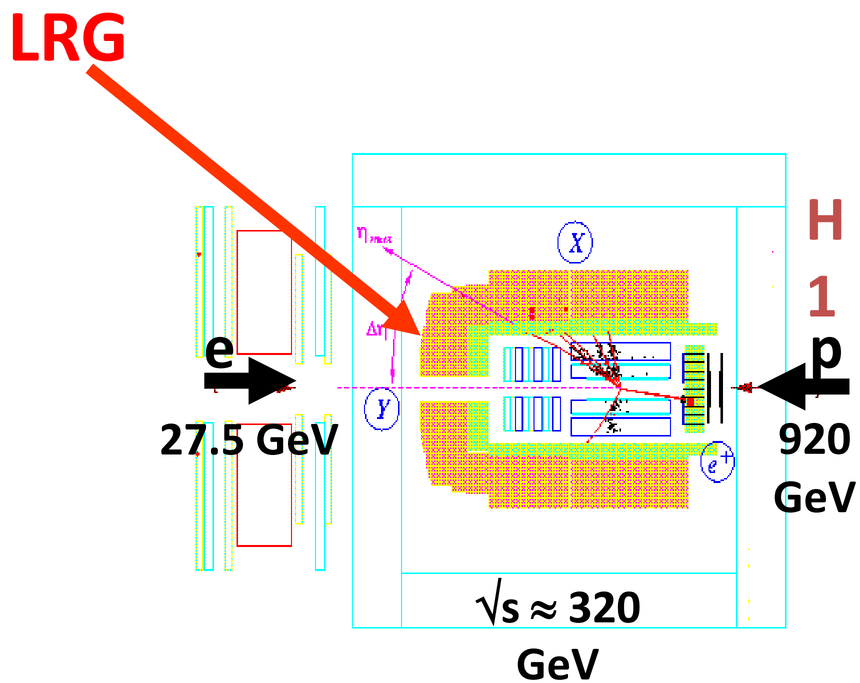

to M_Y<1.6 GeV

•In this method the outgoing proton is not observed, but the diffractive nature of the event is inferred from the presence of a large gap in the rapidity distribution of the final state hadrons.

•This method has the advantage of a large acceptance yielding high statistical data samples.

•It has the disadvantage that the selected data sample contains, in certain kinematical regions, contributions from non-diffractive processes and from proton dissociation.

Forward Proton Spectrometer (FPS) or Roman Pot Method

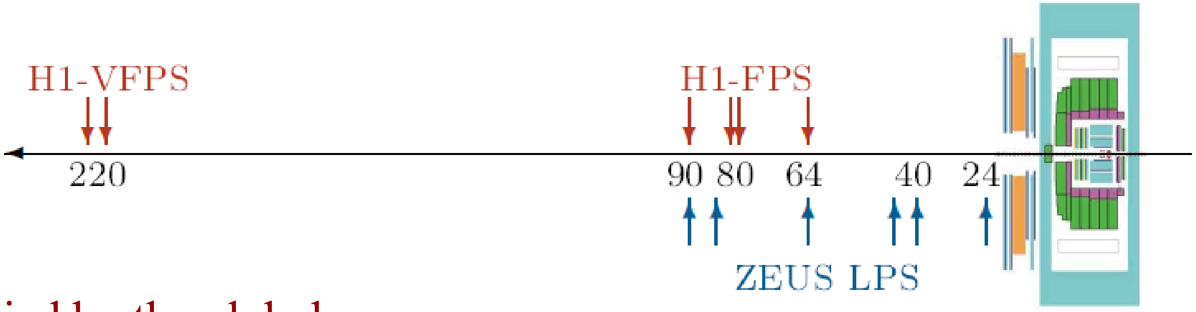

Data multiplied by the global factor 1.23, 1.33 and 1.2

The diffractively scattered proton are detected directly in detectors housed in movable stations called Roman Pots. The Roman Pot devices are known as the LPS in the case of ZEUS and the FPS in H1.

This method has the advantages of providing the cleanest separation between elastic, proton dissociative and non-diffractive events.

The disadvantage of the method is its small acceptance which gives more restricted samples in terms of kinematic coverage. This is why we use them only in global fits with all available data sets.

A. Aktas *et al.* [H1 Collaboration], Eur. Phys. J. C **48**, 749 (2006) [arXiv:hep-ex/0606003].

S. Chekanov [ZEUS Collaboration], Nucl. Phys. B **800**, 1 (2008) [arXiv:0802.3017 [hep-ex]].

H. Collaboration, arXiv:1010.1476 [hep-ex].

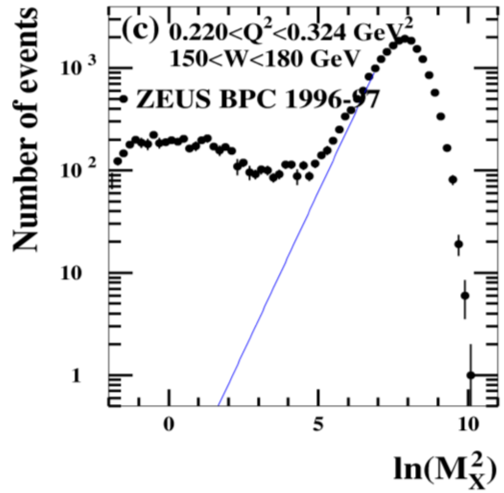

Data multiplied by the global factor 0.86

Again the outgoing proton is not observed, but rather than requiring a large rapidity gap, diffractive events are selected on the basis of differences in the shape of the invariant mass distribution of the final state particles seen in the detector for non-diffractive and diffractive events

The advantage of MX method is that it removes non-diffractive background and that its acceptance is high.

However, like the large rapidity gap method, this method allows contributions from proton dissociative events.

S. Chekanov *et al.* [ZEUS Collaboration], Eur. Phys. J. C **38**, 43 (2004) [arXiv:hep-ex/0408009].

S. Chekanov *et al.* [ZEUS Collaboration], Nucl. Phys. B **816**, 1 (2009) [arXiv:0812.2003 [hep-ex]].

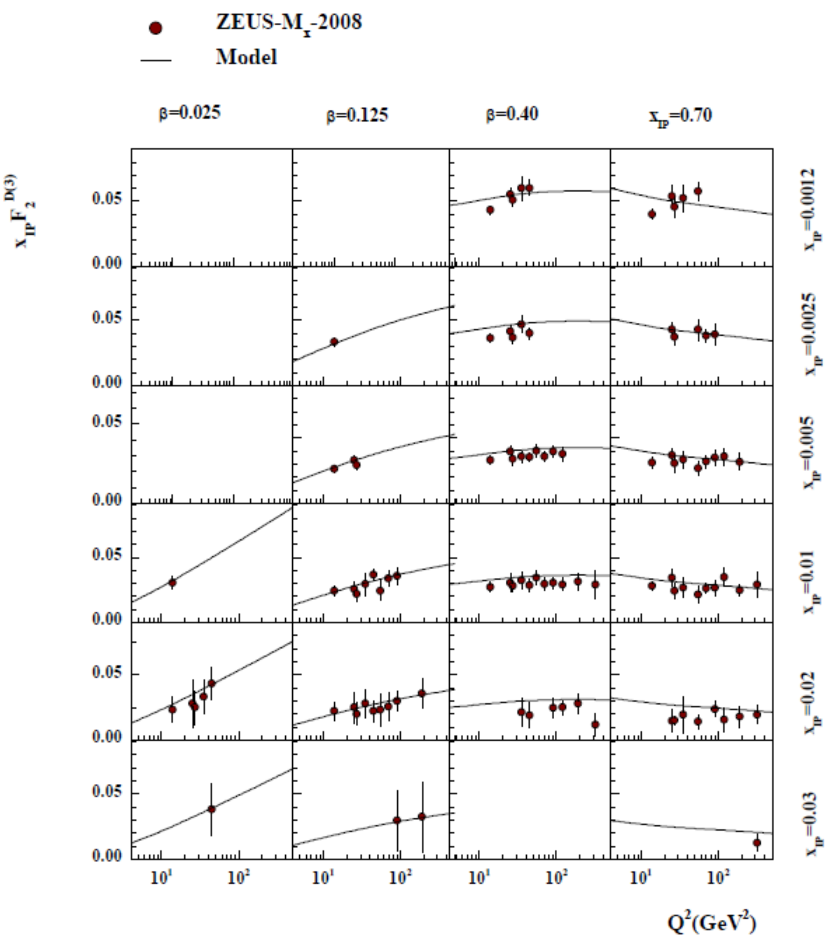

The diffractive cross section of the proton multiplied by x_{IP} , as a function of Q^2 for different regions of x_{IP} and □. The curves show the result of our fit.

S. Chekanov *et al.* [ZEUS Collaboration], Nucl. Phys. B **816**, 1 (2009) [arXiv:0812.2003 [hep-ex]].

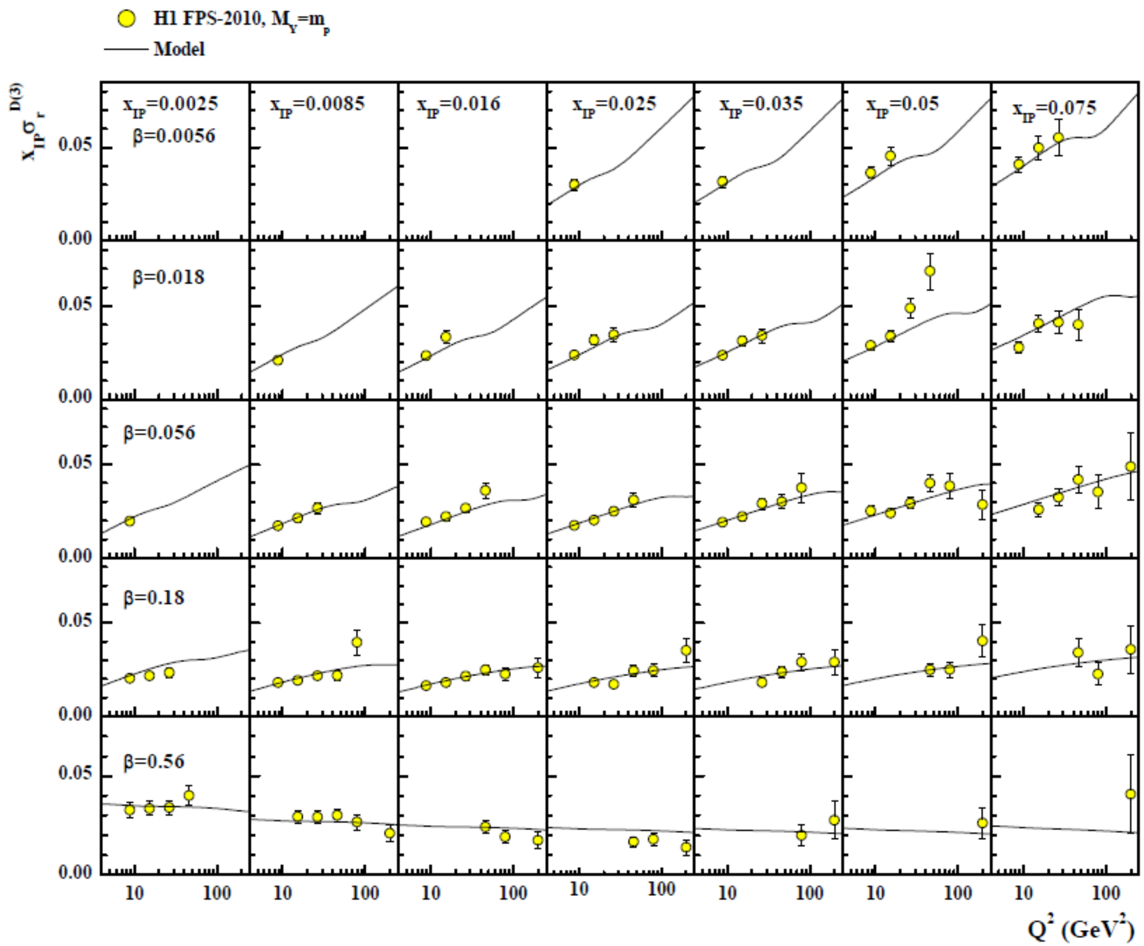

The diffractive cross section of the proton multiplied by x_{IP} , as a function of Q^2 for different regions of x_{IP} and □. The curves show the result of our fit.

H. Collaboration, arXiv:1010.1476 [hep-ex].

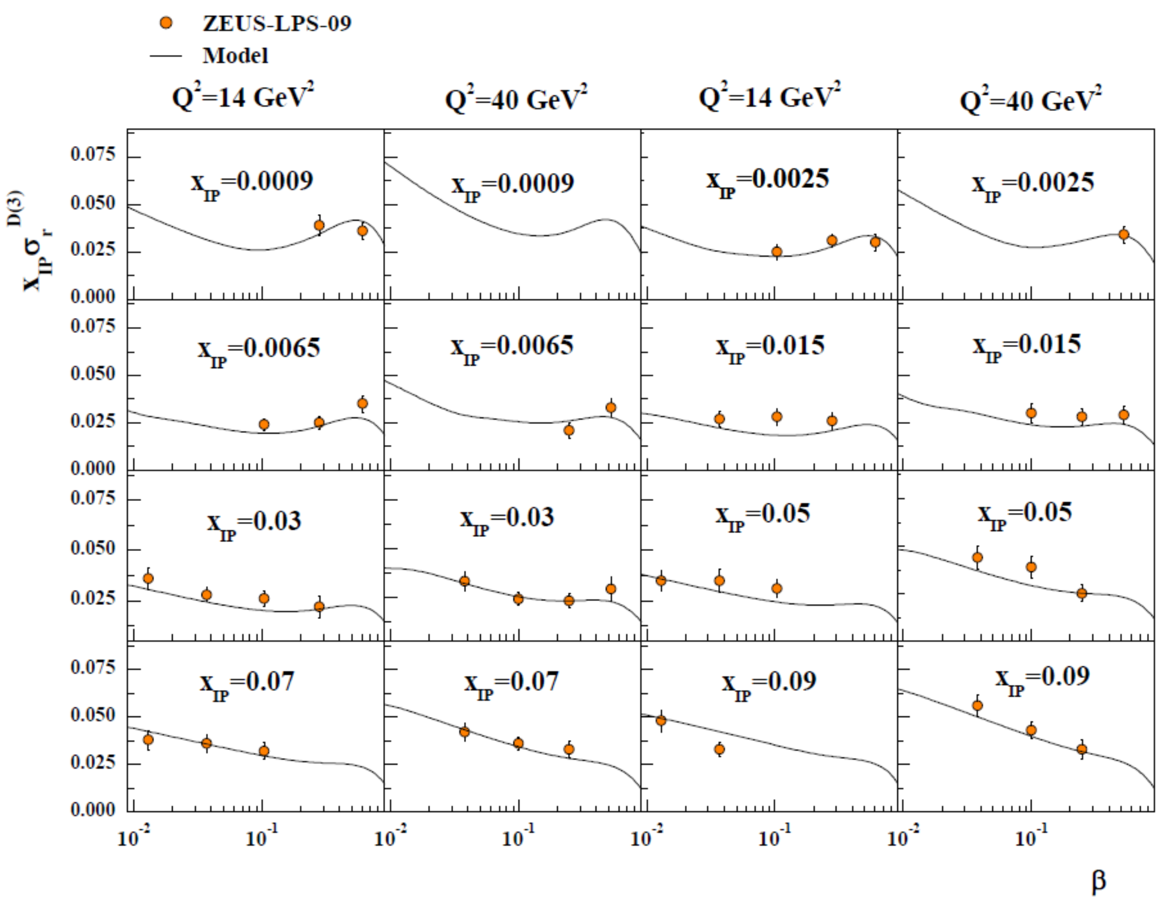

The diffractive cross section of the proton multiplied by x_{IP} , as a function of β for different regions of x_{IP} and Q^2. The curves show the result of our fit.

S. Chekanov [ZEUS Collaboration], Nucl. Phys. B **800**, 1 (2008) [arXiv:0802.3017 [hep-ex]].

QCD Fit – comparison with H1-FPS-06 data

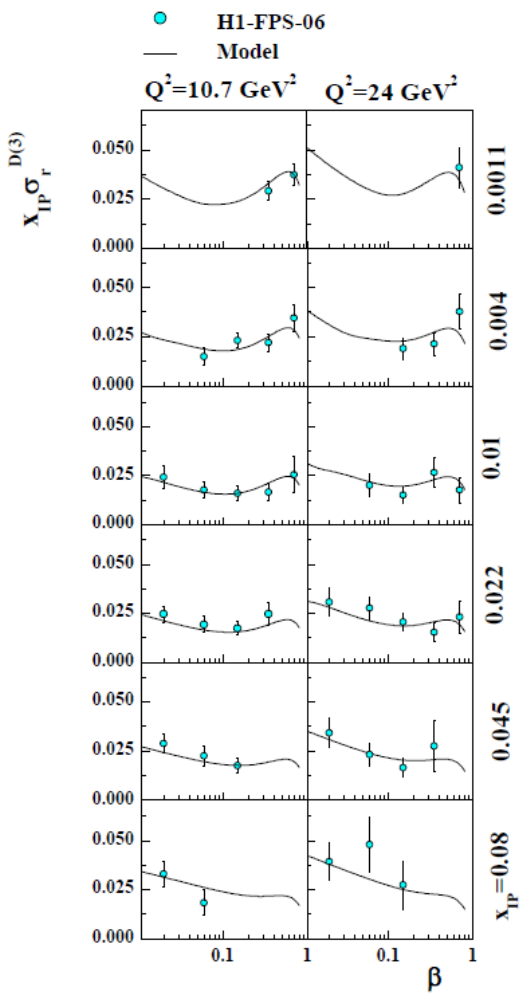

The diffractive cross section of the proton multiplied by x_{IP} , as a function of for different regions of x_{IP} and Q^2. The curves show the result of our fit.

A. Aktas *et al.* [H1 Collaboration], Eur. Phys. J. C 48, 749 (2006) [arXiv:hep-ex/0606003].